Modeling of temperature distribution in a reinforced concrete supertall structure based on structural health monitoring data

Y.Q. Ni*, P. Zhang, X.W. Ye, K.C. Lin and W.Y. Liao

Department of Civil and Structural Engineering
The Hong Kong Polytechnic University, Hung Hom, Kowloon, Hong Kong

Abstract. A long-term structural health monitoring (SHM) system comprising over 700 sensors of sixteen types has been implemented on the Guangzhou Television and Sightseeing Tower (GTST) of 610 m high for real-time monitoring of the structure at both construction and service stages. As part of this sophisticated SHM system, 48 temperature sensors have been deployed at 12 cross-sections of the reinforced concrete inner structure of the GTST to provide on-line monitoring via a wireless data transmission system. In this paper, the differential temperature profiles in the reinforced concrete inner structure of the GTST, which are mainly caused by solar radiation, are recognized from the monitoring data with the purpose of understanding the temperature-induced structural internal forces and deformations. After a careful examination of the pre-classified temperature measurement data obtained under sunny days and non-sunny days, common characteristic of the daily temperature variation is observed from the data acquired in sunny days. Making use of 60-day temperature measurement data obtained in sunny days, statistical patterns of the daily rising temperature and daily descending temperature are synthesized, and temperature distribution models of the reinforced concrete inner structure of the GTST are formulated using linear regression analysis. The developed monitoring-based temperature distribution models will serve as a reliable input for numerical prediction of the temperature-induced deformations and provide a robust basis to facilitate the design and construction of similar structures in consideration of thermal effects.

Keywords: structural health monitoring; supertall structure; reinforced concrete; temperature effect; temperature distribution model; least-squares regression analysis.

1. Introduction

In recent years, numerous supertall structures for commercial and residential functions have been built or are being constructed in many densely urbanized cities in China. In addition to wind-induced dynamic response, slender structures such as television towers, industrial chimneys, and high-rise buildings are prone to temperature-induced quasi-static deformation as subjected to diurnal or seasonal temperature fluctuations. Considerable temperature differences may occur among adjacent structural members under certain climatological conditions and result in notable structural internal forces and deformations due to the restraints. Specifically, the structural members exposed to direct solar radiation will be at a higher temperature than those on the opposite shaded side, and the structure will thus tend to deflect away from the sun. In some situations, the temperature-

---

* Corresponding author, Professor, E-mail: ceyqni@polyu.edu.hk

induced deflection at the top of a supertall structure can reaches over 20% of the drift caused by wind forces (Smith and Coull 1991). Therefore, it becomes essential and desirable to investigate the variational characteristics and statistical patterns of the structural temperature distribution for properly analyzing the structural behavior in consequence of thermal effects.

Research efforts have been devoted to investigating temperature effects on the structural performance and dynamic characteristics of either high-rise structures or long-span bridges. Pirner and Fischer (1999) conducted the measurement of stresses due to insolation ascertained on the Prague TV tower and concluded that stresses due to temperature changes were not of negligible magnitude. The temperature distribution on the external surface of the Stuttgart TV Tower has been recognized and the daily and seasonal drift of the tower top due to solar radiation and the daily air temperature variation have been acquired (Breuer *et al.* 2008). Ni *et al.* (2009b) investigated the temperature-induced deformation of the GTST based on a precise 3D finite element model (FEM) of the structure, and the predicted deformations were compared with the measurement results obtained by a global positioning system (GPS). DeWolf *et al.* (1995) studied the interaction between the variable temperature and the governing natural frequencies of a two-span composite steel-girder bridge and a curved post-tensioned bridge (Liu and DeWolf 2007). Sohn *et al.* (1999) conducted an experimental study of temperature effect on modal parameters of the Alamosa Canyon Bridge. Also, extensive investigations on the modeling of temperature effects on modal frequencies for the cable-supported bridges and the establishment and checking of the temperature-displacement pattern of bridge expansion joints have been conducted by use of long-term monitoring data (Ni *et al.* 2005, Hua *et al.* 2007, Ni *et al.* 2007). However, only little attention has been given to the accurate description and modeling of temperature distribution for in-construction and/or in-service high-rise concrete structures.

Long-term SHM, enabled by recent advances in sensing and data acquisition technologies, communication algorithms, computational techniques, and data management systems, has gained worldwide applications in civil engineering field (Ko and Ni 2005, Brownjohn 2007). Developing long-term SHM systems for large-scale civil engineering structures is able to provide thorough and most reliable information for evaluating structural integrity, durability and reliability throughout the life-cycle and for ensuring optimal maintenance planning and safe operation. The GTST located in the city of Guangzhou, China, is a tube-in-tube structure with a total height of 610 m. This supertall structure is deemed to be sensitive to temperature and prone to vibration. In order to assess the structural safety, a sophisticated long-term SHM system has been implemented in parallel with the construction progress for on-line monitoring of the GTST at both construction and service stages. A total of 48 temperature sensors have been deployed at 12 selected cross-sections of the reinforced concrete inner structure of the GTST to provide real-time temperature monitoring via a wireless data transmission system. In this paper, the differential temperature profiles in the reinforced concrete inner structure of the GTST, which are mainly caused by solar radiation, are analyzed using the monitoring data. With a careful examination of the pre-classified temperature measurement data obtained under sunny days and non-sunny days, common characteristic of the daily temperature variation is identified from the data acquired in sunny days. Making use of 60-day temperature measurement data obtained in sunny days, statistical patterns of the daily rising temperature and daily descending temperature are synthesized, and temperature distribution models of the reinforced concrete inner structure of the GTST are formulated using a least-squares regression analysis method.

2. GTST and its SHM system

The GTST is a concrete-steel composite structure as shown in Fig. 1. The main tower of 454 m high comprises a reinforced concrete inner structure with an ellipse cross-section of 14 m × 17 m and a steel lattice outer structure with its cross-section being a varying oval which decreases from 50 m × 80 m at the ground to the minimum of 20.65 m × 27.5 m at the height of 280 m (waist level), and then increases to 41 m × 55 m at the top of the main tower (454 m). There are 37 floors connecting the inner and outer structures that serve for various functions, e.g. television and radio transmission facilities, observatory decks, Ferris wheels, exhibition spaces, shops, revolving restaurants, conference rooms, computer gaming, and 4D cinemas. The antenna mast of 156 m high founded on the main tower is a steel spatial structure with an octagonal cross-section of 14 m in the maximum diagonal.

2.1 SHM system for GTST

A long-term SHM system has been implemented on the GTST by a team from The Hong Kong

(a) GTST under construction   (b) Outer steel structure   (c) Inner concrete structure
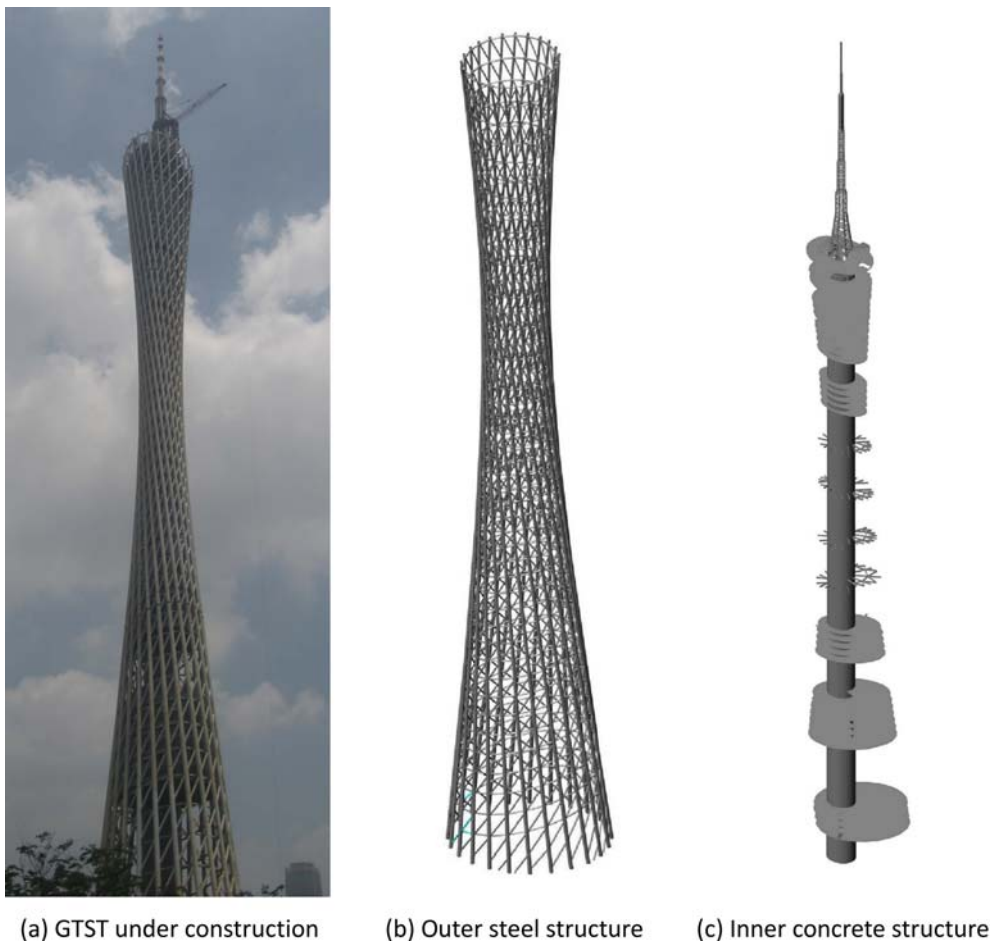
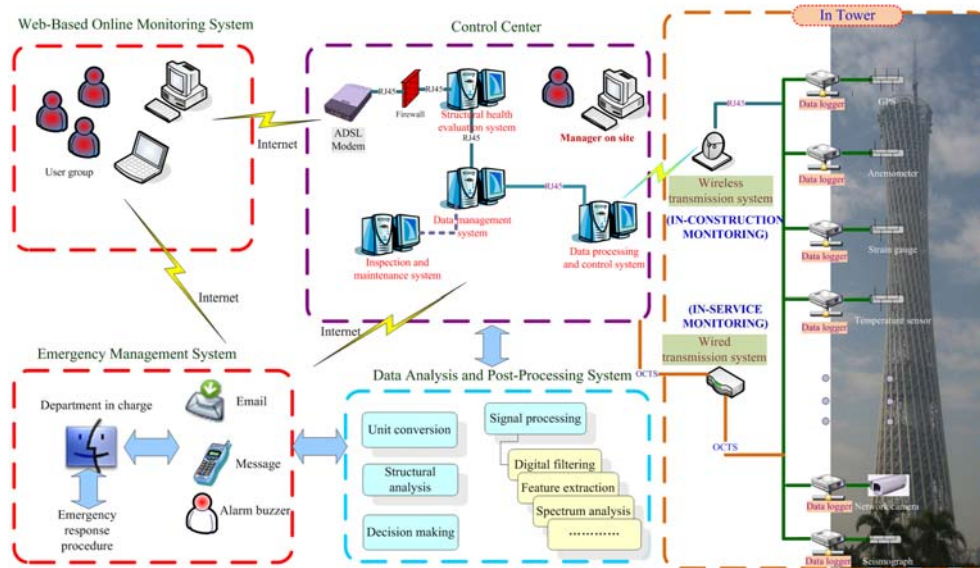Fig. 1 Guangzhou Television and Sightseeing Tower (GTST)

Fig. 2 Topology of integrated in-construction and in-service monitoring system

Polytechnic University. As shown in Fig. 2, it exercises a pioneering SHM practice of integrating in-construction monitoring and in-service monitoring (Ni *et al.* 2009a). Through FEM-based structural analysis, 12 cross-sections at construction stage and 5 cross-sections at service stage have been selected for the installation of over 700 sensors. This on-line SHM system has been devised based on the modular design concept and consists of six functional modules: (i) Sensory System (SS), (ii) Data Acquisition and Transmission System (DATS), (iii) Data Processing and Control System (DPCS), (iv) Structural Health Data Management System (SHDMS), (v) Structural Health Evaluation System (SHES), and (vi) Inspection and Maintenance System (IMS). The SS and DATS are located in the structure, the DPCS, SHDMS and SHES are inside the monitoring center room, and the IMS is a portable system.

The SS is composed of 16 types of sensors which include a weather station, a total station, zenithal telescopes, theodolites, wind pressure sensors, vibrating wire strain gauges, thermometers, accelerometers, level sensors, tiltmeters, corrosion sensors, digital video cameras, fiber optic dynamic strain and temperature sensors, a seismograph, and a GPS. Crucial information including environmental effects (temperature, humidity, rain, air pressure, and corrosion), loading sources (wind, seismic, and thermal loading), and structural responses (strain, displacement, inclination, acceleration, and geometric configuration) can be acquired in real time. The DATS consists of 13 stand-alone data acquisition units (DAUs) (sub-stations) for in-construction monitoring and 6 stand-alone DAUs (sub-stations) for in-service monitoring. The DAUs are assigned at several cross-sections of the GTST to collect the signals from surrounding sensors, digitize the analog signals, and transmit the data into a central room in either wired or wireless manner. The DPCS comprises high-performance servers located in the central room and data-processing software. It is devised to control the on-structure DAUs regarding data acquisition and pre-processing, data transmission and filing, and display of the data. The DMS comprises an Oracle-driven database system for non-spatial temporal data management and a Geographic Information System (GIS) software system for spatial data management. The SHES is composed of an on-line structural condition evaluation system and

an off-line structural health and safety assessment system. The IMS is a laptop-computer-aided portable system for inspecting and maintaining sensors, DAUs, and cabling networks.

2.2 Deployment of temperature sensors

Fig. 3 illustrates the deployment of temperature sensors on the reinforced concrete inner structure of the GTST. A total of 12 cross-sections of the reinforced concrete inner structure have been selected for temperature monitoring. They are at the levels of 32.8 m, 100.4 m, 121.2 m, 173.2 m, 204.4 m, 230.4 m, 272.0 m, 303.2 m, 334.4 m, 355.2 m, 376.0 m, and 433.2 m high, and designated as section 1 to section 12, respectively. The selected cross-sections are expected to suffer large stresses under certain construction and in-service loadings or experience an abrupt change in lateral stiffness. They were determined by finite element analysis of the structure at critical construction stages and the completed stage. Each monitoring section includes 4 temperature sensors (together with strain gauges) as illustrated in Fig. 3(b). The surface-type temperature sensors for

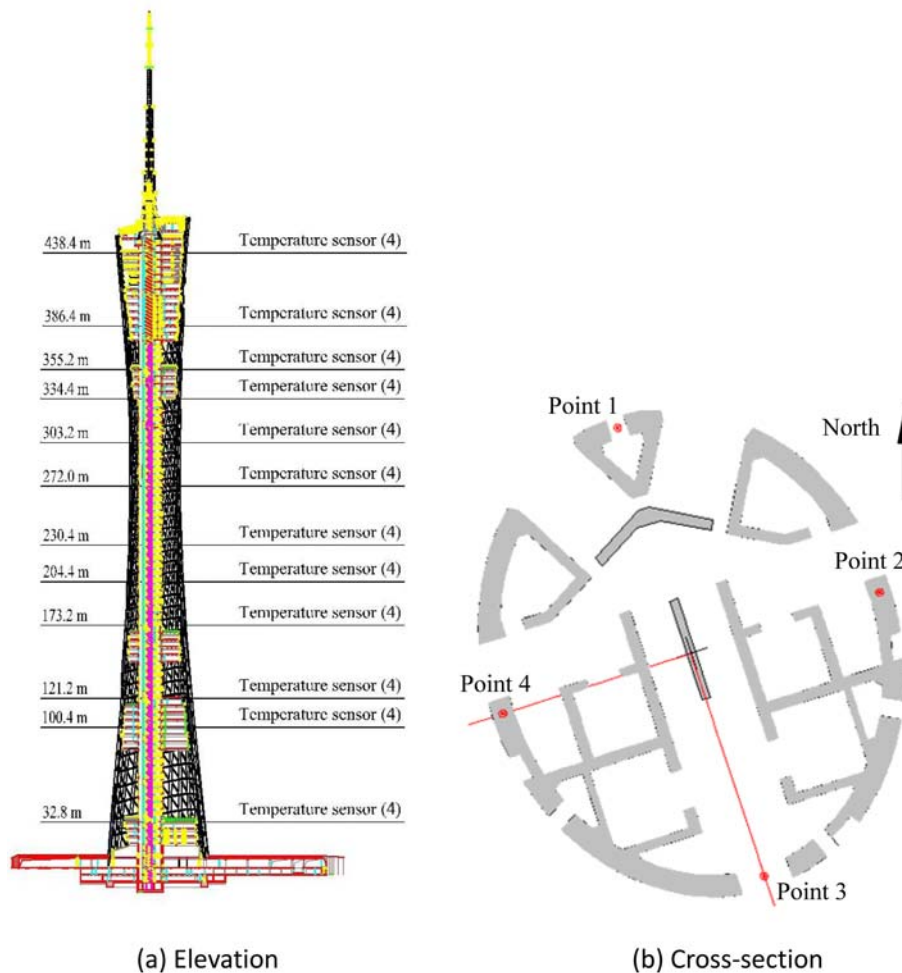

(a) Elevation   (b) Cross-section

Fig. 3 Deployment of temperature sensors on reinforced concrete inner structure

sections 1 and 2 were attached on the outer surface of the reinforced concrete core (because these two sections had been erected when implementing the SHM system), while the embedment-type temperature sensors for the other sections were installed at the center of the concrete wall thickness in synchronism with the construction progress for measuring the temperature inside concrete. It is worth mentioning that there are several functional floors of connecting the inner and outer structures which cover the zones of sections 1 and 2 as well as between sections 9 and 12, so that the solar radiation cannot directly reach the inner structure at the regions with functional floors. A wireless system has been developed for synchronous acquisition of temperature data of the reinforced concrete inner structure and real-time data transmission from the data acquisition units (sub-stations) to the site office during the construction period. The sampling rate for each sensor is set as one data per minute in normal circumstances and can be switched to one data per second during typhoons and other extreme events.

3. Temperature measurement data and preliminary analysis

Up to the end of September 2008, the GTST has been erected to the height of 454 m with the completion of the reinforced concrete inner structure. Temperature data of the 12 monitoring sections were acquired and transmitted automatically by the SHM system. Fig. 4 shows the measured temperature time histories for point 1 on section 6 of the reinforced concrete inner structure and for surrounding air, covering 8 months from 1st October 2008 to 31st May 2009. The temperature data for the surrounding air were provided by Guangdong Meteorological Administration, of which the sampling rate is one data per half an hour with a resolution of 1°C. It is observed from Fig. 4 that the overall profile and variation tendency of the measured temperature inside the reinforced concrete inner structure coincides well with that of the surrounding air temperature, while the range of daily temperature variation inside the reinforced concrete inner structure is much less than that of the surrounding air. In the following, the temperature measurement data obtained under sunny days and non-sunny days are examined separately.

3.1 Temperature data in sunny days

A total of 60-day temperature data acquired in sunny days during the period from October 2008 to May 2009 are adopted in the present study. Fig. 5 shows the measured temperatures of the 4 points on section 6 inside the reinforced concrete inner structure and the surrounding air during 20th and 21st October 2008. It is observed that the measured temperatures for both the reinforced
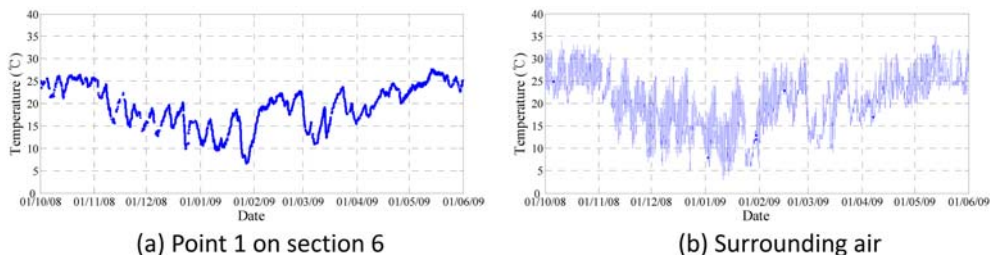

(a) Point 1 on section 6   (b) Surrounding air

Fig. 4 Measured temperature time histories covering 8 months

(a) Points 1 to 4 on section 6   (b) Surrounding air
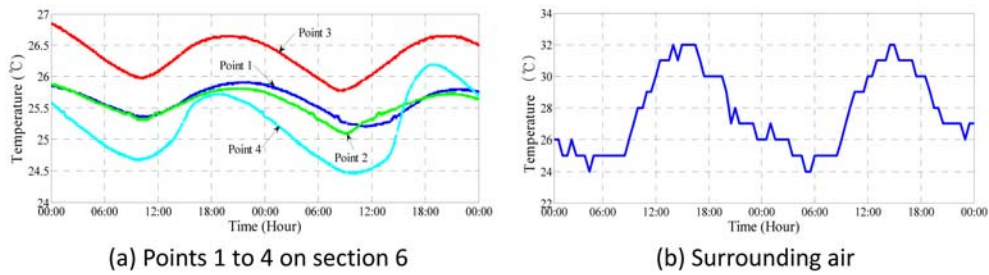
Fig. 5 Measured temperatures during 20th and 21st October 2008

concrete inner structure and the surrounding air vary with a well-regulated mode in the two days, and there exists an obvious temperature variation pattern which consists of a temperature rising phase and a temperature descending phase. Another observation from Fig. 5 is that the measured temperature of the reinforced concrete inner structure varies gently with a delay in comparison with the temperature variation of the surrounding air. This is mainly because the reinforced concrete inner structure is not entirely exposed to the surroundings and a certain period of time is required for temperature infiltration into the concrete from the structural surface. The amplitudes of daily temperature fluctuation of the reinforced concrete inner structure and the surrounding air are approximately 1ºC and 8ºC, respectively.

3.2 Temperature data in non-sunny days

Fig. 6 shows the measured temperatures of the 4 points on section 6 inside the reinforced concrete inner structure and the surrounding air in two non-sunny days that were cloudy on 23rd March 2009 and rainy on 24th March 2009. By contrast to the temperature data acquired in sunny days, it is found difficult to capture a regular trend of temperature variation from the measurement data acquired in non-sunny days for both the reinforced concrete inner structure and the surrounding air. In Fig. 6(b), it is seen that the amplitude of daily temperature fluctuations of the surrounding air on 23rd March 2009 is 6ºC, which is 2ºC less than that observed in the sunny days. On the early morning of 24th March 2009, there was a rain in the city of Guangzhou where the GTST is located, and the measured temperature of the surrounding air declined sharply and began to rise until the rain stopped.

Strong winds buffeted the city of Guangzhou during the period from 23rd to 25th January 2009, the maximum wind velocity was measured 11 m/s and the wind directions are north and northeast.
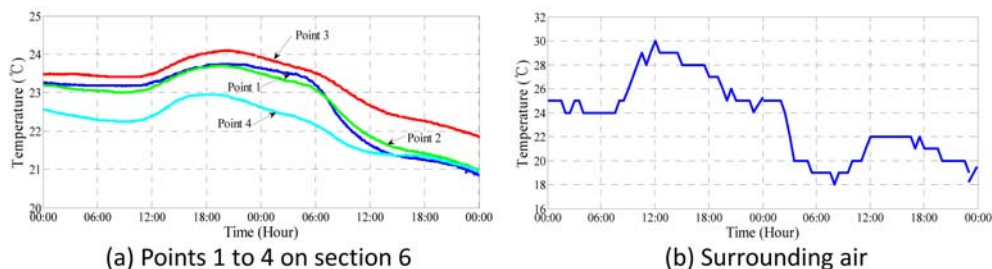

(a) Points 1 to 4 on section 6   (b) Surrounding air

Fig. 6 Measured temperatures during 23rd and 24th March 2009

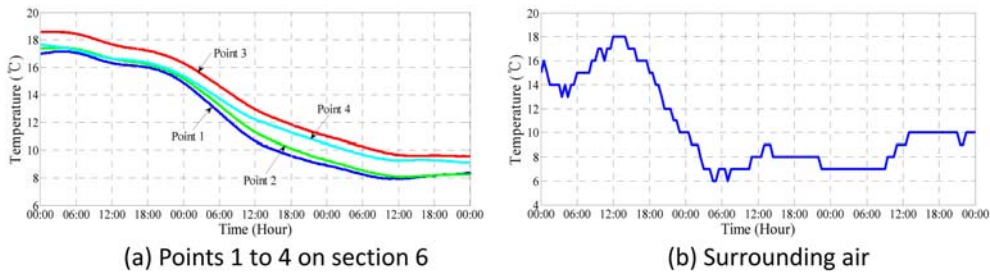(a) Points 1 to 4 on section 6   (b) Surrounding air

Fig. 7 Measured temperatures during 23rd and 25th January 2009

Fig. 7 shows the measured temperatures of the 4 points on section 6 inside the reinforced concrete inner structure and the surrounding air during 23rd and 25th January 2009. It is found from Fig. 7 that the measured temperature of the surrounding air dropped abruptly from 18ºC at 01:00 pm on 23rd January 2009 to 6ºC at 06:00 am on 24th January 2009, while the temperature of the reinforced concrete inner structure declined slowly.

4. Temperature distribution models

According to the observations of the measured temperature data as described in the previous section, a temperature variation pattern for sunny days has been identified which can be characterized by a temperature rising phase and a temperature descending phase. Temperature distribution models of the reinforced concrete inner structure are accordingly formulated based on the measured sunny-day temperature data from the SHM system of the GTST.

4.1 Feature extraction from measured temperature data

The differential temperature profile in the reinforced concrete inner structure is mainly caused by solar radiation, and it fluctuates regularly along with the ambient environment in a normal sunny day. A typical sunny-day measured temperature time history of point 3 on section 6 is illustrated in Fig. 8. It can be observed that the temperature time history exhibits an obvious trend with a
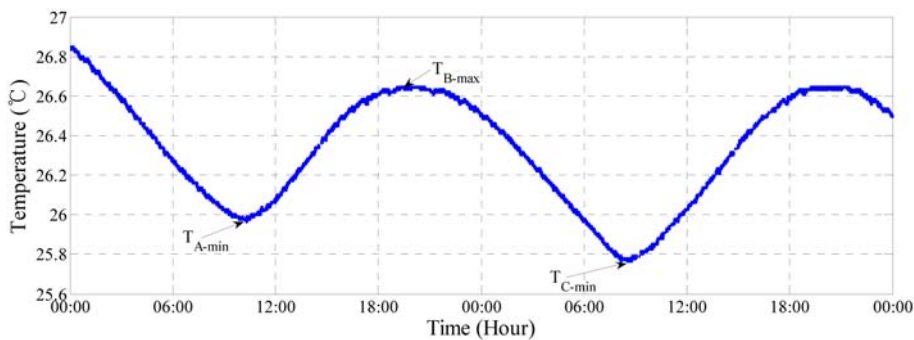

Fig. 8 Measured temperatures at point 3 on section 6

temperature rising phase and a temperature descending phase within a time period of 24 hours. The temperature approximately attains its daily minimum at 10:00 am and its daily maximum at 7:00 pm. Thus, two variables, namely the daily rising temperature and the daily descending temperature, can be defined to explore the features of temperature distribution inside the reinforced concrete inner structure. They are expressed by

$$T_r = T_{B\_max} - T_{A\_min} \qquad (1)$$

$$T_d = T_{C\_min} - T_{B\_max} \qquad (2)$$

in which T_r and T_d denote the daily rising and descending temperatures, respectively; T_{B_max} represents the daily peak temperature, and T_{A_min} and T_{C_min} are the two adjacent troughs around the peak temperature. With the 60-day temperature data of the reinforced concrete inner structure acquired in sunny days, the values of the rising temperature and the descending temperature are procured during October 2008 and May 2009, and statistically analyzed in the following.

4.2 Statistical analysis

Fig. 9 shows the probability distributions of the daily rising and descending temperatures acquired at point 3 on section 6 inside the reinforced concrete inner structure. By conducting a hypothesis test (Montgomery *et al.* 2007), it is testified that the daily rising and descending temperatures follow normal distribution at 5% level of significance. The mean values of the daily rising and descending temperatures at the 4 points on all 12 cross-sections of the reinforced concrete inner structure are demonstrated in Figs. 10 to 12.

From Figs. 10 to 12, it is observed that (i) the temperature distribution on sections 1 and 2 shows a profile different from that on the other sections, and it is attributed to the fact that the temperature sensors on sections 1 and 2 are attached on the surface of the reinforced concrete inner structure while the embedment-type temperature sensors are adopted for the other sections; (ii) for each monitoring section exclusive of sections 1 and 2, the amplitudes of temperature variation at points 2 to 4 are relatively larger than those at point 1 which is located in the shady side of the inner structure; and (iii) temperature variation on the sections without connection to the functional floors is relatively larger than that on the sections with connection to the functional floors, and the

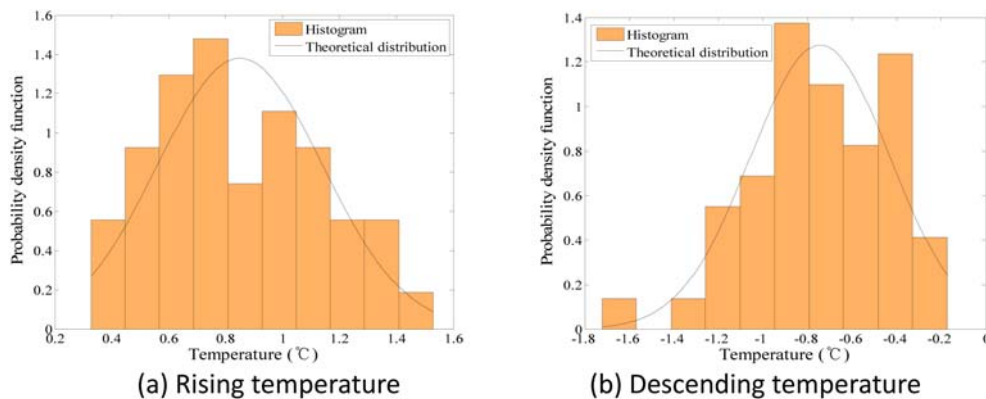(a) Rising temperature   (b) Descending temperature

Fig. 9 Probability distributions of daily rising and descending temperatures at point 3 on section 6
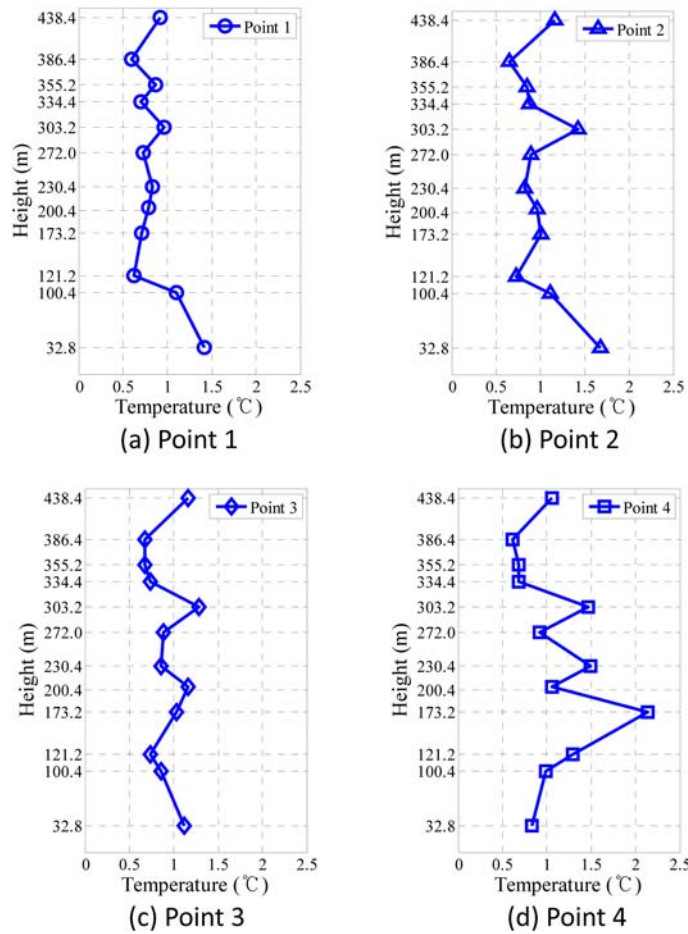
Fig. 10 Mean values of daily rising temperatures along elevation

maximum temperature variation occurs at the middle waist level of the tower.

4.3 Formulation of temperature distribution models

Taking full advantage of the above observations, the reinforced concrete inner structure is sectionalized into three segments along elevation according to the sectional deployment of temperature sensors. The first segment is termed the bottom segment with a range from sections 1 to 4, in which the measured temperature from sections 1 and 2 attached with the surface-type temperature sensors approximately represents the temperature of surrounding environment. While sections 3 and 4 are separately located on the roof gardens of the functional floors B and C, the measured temperature from these two sections has a similar temperature variation pattern. As a result, the mean value of the measured temperatures from sections 3 and 4 is defined as the temperature of the bottom segment with its height coverage from 0.0 m to 188.8 m. The second segment is the waist segment covering from sections 5 to 8 located in the waist of the GTST, and the temperature of the waist segment is defined by averaging the temperature data acquired from sections 5 to 8 ranging between 188.8 m and 318.8 m in height. The last segment is named the top
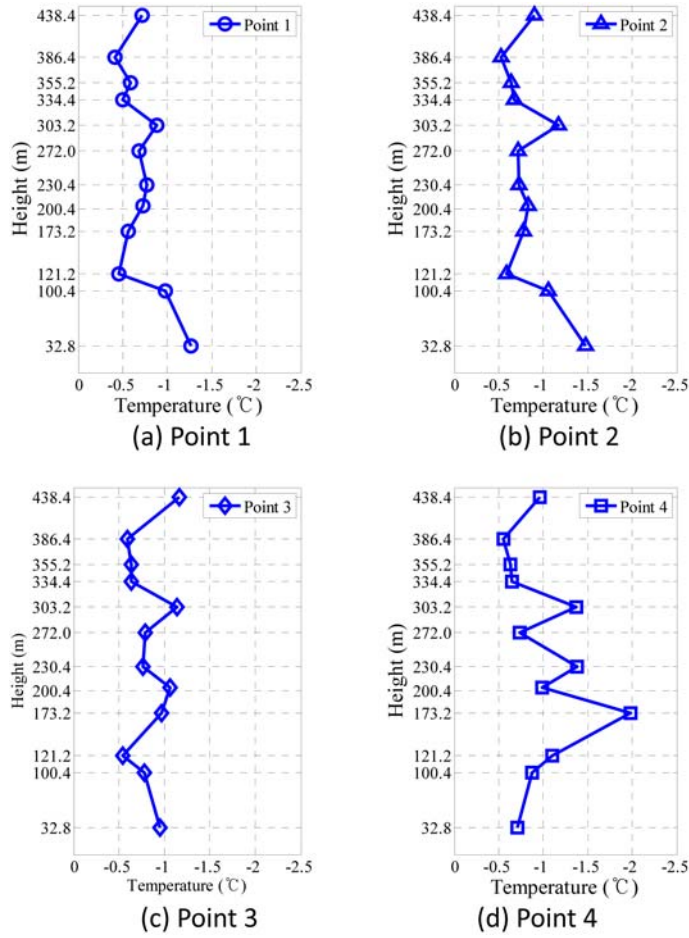
Fig. 11 Mean values of daily descending temperatures along elevation

segment which includes sections 9 to 12 ranging between 318.8 m and 448.8 m in height, and the temperature of the top segment is defined by averaging the temperature data acquired from sections 9 to 12. The variables which represent the daily rising temperature and the daily descending temperature of these three defined segments are defined as

$$T_{bri} = \frac{T_{3ri} + T_{4ri}}{2} \tag{3}$$

$$T_{wri} = \frac{T_{5ri} + T_{6ri} + T_{7ri} + T_{8ri}}{4} \tag{4}$$

$$T_{tri} = \frac{T_{9ri} + T_{10ri} + T_{11ri} + T_{12ri}}{4} \tag{5}$$
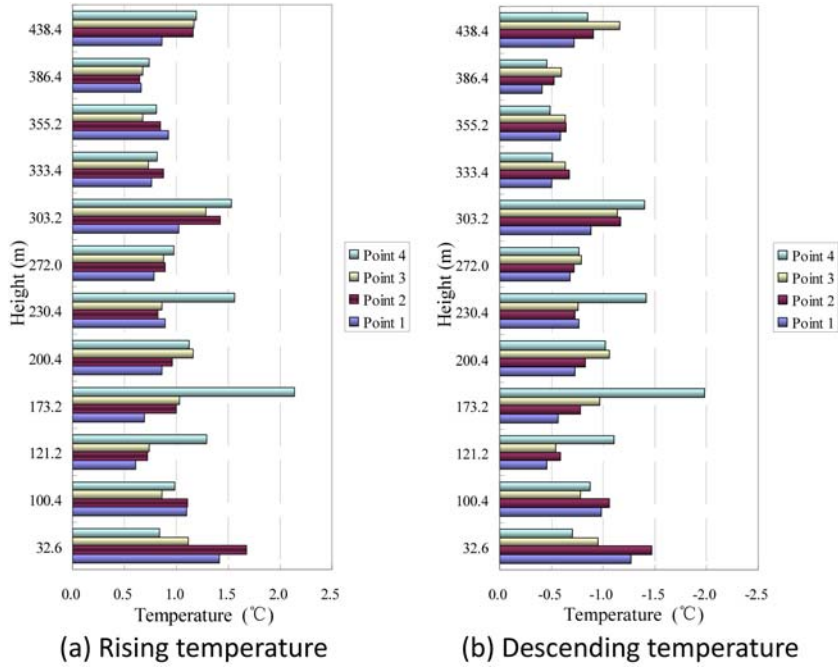
$$T_{bdi} = \frac{T_{3di} + T_{4di}}{2} \tag{6}$$

Fig. 12 Mean values of daily rising and descending temperatures on cross-sections

$$T_{wdi} = \frac{T_{5di} + T_{6di} + T_{7di} + T_{8di}}{4} \tag{7}$$

$$T_{tdi} = \frac{T_{9di} + T_{10di} + T_{11di} + T_{12di}}{4} \tag{8}$$

where i denotes the number of the monitoring point; T_{bri} and T_{bdi} are the daily rising and descending temperatures of the bottom segment; T_{wri} and T_{wdi} are the daily rising and descending temperatures of the waist segment; T_{tri} and T_{tdi} are the daily rising and descending temperatures of the top segment; and the variables T_{3ri} to T_{12ri} and T_{3di} to T_{12di} are the daily rising temperatures and the daily descending temperatures obtained on sections 3 to 12.

4.3.1 Linear regression analysis

In order to explore the correlations among the daily rising temperatures and among the daily descending temperatures of the three defined segments, the least-squares regression analysis (Keller 2009) is carried out. As an example, the correlation pattern between T_{br2} and T_{wr2} is formulated by use of the 60-day temperature measurement data of point 2 acquired in sunny days during the period from October 2008 to May 2009. Fig. 13 plots the correlation between T_{br2} and T_{wr2}, with which a linear regression model is obtained as

$$T_{br2} = 0.113 + 0.718 T_{wr2} \tag{9}$$

The sum of squared errors (SSE) is calculated by
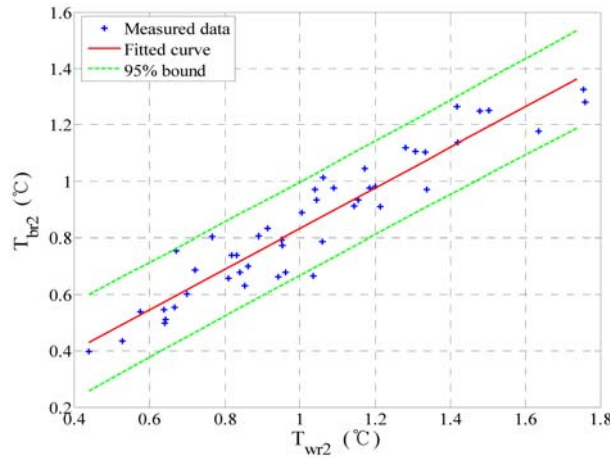
Fig. 13 Correlation between T_{wr2} and T_{br2}

$$SSE = \sum_{i=1}^{n}(y_i - \hat{y}_i)^2 \tag{10}$$

where y_i is the sample data of T_{br2}; and $\hat{y}_i$ is the estimator of y_i.

The coefficient of determination, R^2 is obtained by

$$R^2 = 1 - \frac{SSE}{\sum(y_i - \bar{y})^2} \tag{11}$$

where $\bar{y}$ represents the mean value of y_i.

The value of R^2 for the linear regression model in Eq. (9) is obtained as 0.944, indicating that T_{br2} is almost linearly with T_{wr2}.

4.3.2 Temperature distribution models

The linear regression models of the daily rising temperatures and the daily descending temperatures among T_{bri}, T_{bdi}, T_{wri}, T_{wdi}, T_{tri}, and T_{tdi} are obtained and demonstrated in Tables 1 and 2. The regression coefficients β_0 and β_1, and the coefficient of determination R^2 of the linear

Table 1 Correlation among daily rising temperatures

Point No.	x	y	β_0	β_1	R^2
1	T_{wr1}	T_{br1}	0.013	0.743	0.937
		T_{tr1}	-0.290	0.989	0.822
2	T_{wr2}	T_{br2}	0.107	0.718	0.944
		T_{tr2}	-0.016	0.647	0.750
3	T_{wr3}	T_{br3}	0.113	1.062	0.811
		T_{tr3}	-0.327	0.981	0.826
4	T_{wr4}	T_{br4}	-0.237	1.313	0.844
		T_{tr4}	-0.135	0.683	0.714

Table 2 Correlation among daily descending temperatures

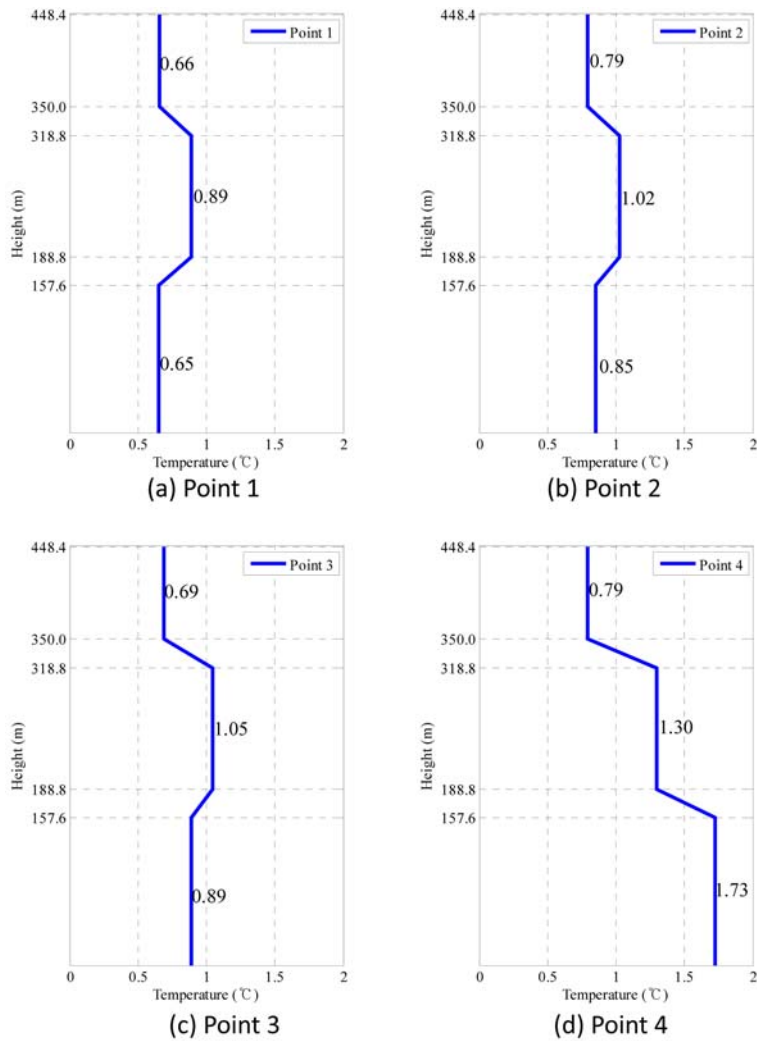| Point No.	x	y	β_0	β_1	R^2
1	T_{wd1}	T_{bd1}	-0.006	0.668	0.896
		T_{td1}	0.280	1.009	0.893
2	T_{wd2}	T_{bd2}	-0.007	0.786	0.905
		T_{td2}	0.090	0.806	0.777
3	T_{wd3}	T_{bd3}	0.090	0.908	0.764
		T_{td3}	0.225	0.851	0.860
4	T_{wd4}	T_{bd4}	-0.178	1.219	0.907
		T_{td4}	0.196	0.560	0.801

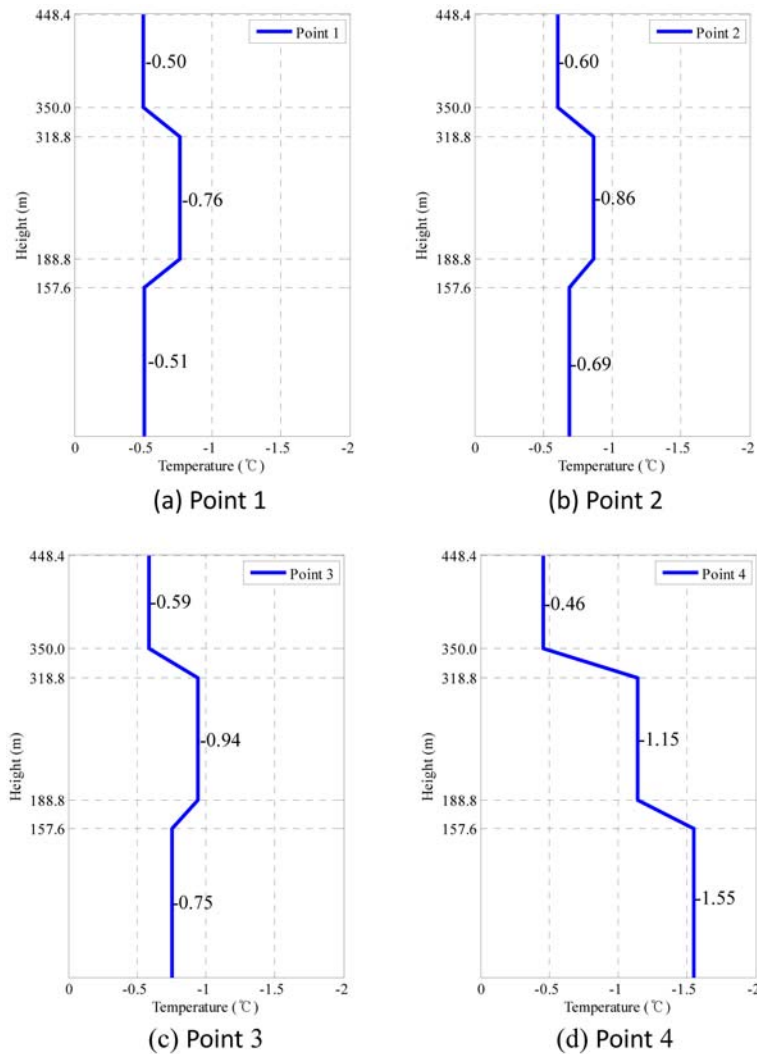Fig. 14 Mean values of daily rising temperature for three defined segments

Fig. 15 Mean values of daily descending temperature for three defined segments

regression models, expressed as $y = \beta_0 x + \beta_1$, are listed in the tables.

In general, the coefficient of determination R^2 measures the strength of linear relationship of a regression model. From Tables 1 and 2, it is seen that the obtained values of R^2 for all the models are larger than 0.7 and most of them are even larger than 0.9, indicating close correlations among the daily rising temperatures and among the daily descending temperatures of the three defined segments. Figs. 14 and 15 illustrate the distribution of the mean values of the daily rising and descending temperatures for the three defined segments of the reinforced concrete inner structure along elevation. Two linear transition zones are introduced to ensure a smooth transition amongst the three defined segments, covering the height from 157.6 m to 188.8 m and from 318.8 m to 350.0 m. Four sub-regions of the inner structure and twelve sub-regions of the outer structure are divided along the length of the cross-section, and the temperature at an arbitrary point without measurement is estimated by interpolating the measured temperatures in the same sub-region on the

cross-section. With the formulated temperature distribution models, the daily rising temperature and descending temperature at any of the three segments can be predicted and extrapolated using the data from limited measurement points. Additionally, the developed temperature distribution models can be incorporated into the FEM model of the GTST to estimate the temperature-induced structural deformations and internal forces (Ni *et al.* 2009b).

5. Conclusions

In this study, temperature distribution models for the reinforced concrete inner structure of the GTST have been formulated by use of the monitoring data from a SHM system permanently installed on the structure. The measured temperature data from both the surface-type and embedment-type temperature sensors and the measured temperature data of surrounding air were carefully examined. It is observed that the temperatures measured in sunny days for both the reinforced concrete inner structure and the surrounding air vary with a well-regulated mode, from which a daily temperature variation pattern consisting of a temperature rising phase and a temperature descending phase is obtained. Based on the analysis of the measured temperature data, the reinforced concrete inner structure of the GTST has been divided into three segments along elevation in accordance with the sectional deployment of temperature sensors. Temperature distribution models of the reinforced concrete inner structure are then formulated by using the least-squares regression analysis. The developed monitoring-based temperature distribution models will serve as a reliable input for numerical simulation of the temperature-induced deformations and internal forces and provide a robust basis to facilitate the design and construction of similar structures in consideration of thermal effects.

Acknowledgements

References

Breuer, P., Chmielewski, T., Gorski, P., Konopka, E. and Tarczynski, L. (2008), "The Stuttgart TV tower-displacement of the top caused by the effects of sun and wind", *Eng. Struct.*, **30**(10), 2771-2781.
Brownjohn, J.M.W. (2007), "Structural health monitoring of civil infrastructure", *Philos. T. R. Soc. A*, **365**(1851), 589-622.
DeWolf, J.T., Conn, P.E. and O'Leary, P.N. (1995), "Continuous monitoring of bridge structures", *Proceedings of the International Association for Bridge and Structural Engineering Symposium on Extending the Lifespan of Structures,* San Francisco, USA, 934-940.

Hua, X.G., Ni, Y.Q., Ko, J.M. and Wong, K.Y. (2007), "Modeling of temperature-frequency correlation using combined principal component analysis and support vector regression technique", *J. Comput. Civil Eng. - ASCE*, **21**(2), 122-135.

Keller, G. (2009), *Managerial statistics,* South-Western Cengage Learning, Mason, Ohio, USA.

Ko, J.M. and Ni, Y.Q. (2005), "Technology developments in structural health monitoring of large-scale bridges", *Eng. Struct.*, **27**(12), 1715-1725.

Liu, C. and DeWolf, J.T. (2007), "Effect of temperature on modal variability of a curved concrete bridge under ambient loads", *J. Struct. Eng. - ASCE*, **133**(12), 1742-1751.

Montgomery, D.C., Runger, G.C. and Hubele, N.F. (2007), *Engineering statistics*, John Wiley & Sons, Hoboken, New Jersey, USA.

Ni, Y.Q., Hua, X.G., Fan, K.Q. and Ko, J.M. (2005), "Correlating modal properties with temperature using long-term monitoring data and support vector machine technique", *Eng. Struct.*, **27**(12), 1762-1773.

Ni, Y.Q., Hua, X.G., Wong, K.Y. and Ko, J.M. (2007), "Assessment of bridge expansion joints using long-term displacement and temperature measurement", *J. Perform. Constr. Fac. - ASCE*, **21**(2), 143-151.

Ni, Y.Q., Xia, Y., Liao, W.Y. and Ko, J.M. (2009a), "Technology innovation in developing the structural health monitoring system for Guangzhou new TV tower", *Struct. Control Health Monit.*, **16**(1), 73-98.

Ni, Y.Q., Zhang, P., Ye, X.W., Lin, K.C. and Liao, W.Y. (2009b), "Temperature-induced deformations of reinforced concrete core of a supertall structure: integrating field monitoring data into finite element analysis", *Proceedings of the 1st International Conference on Computational Technologies in Concrete Structures*, Jeju, Korea, 327-339.

Pirner, M. and Fischer, O. (1999), "Long-time observation of wind and temperature effects on TV towers", *J. Wind Eng. Ind. Aerodyn.*, **79**(1-2), 1-9.

Smith, B.S. and Coull, A. (1991), *Tall building structures: analysis and design*, Wiley, New York, USA.

Sohn, H., Dzwonczyk, M., Straser, E.G., Kiremidjian, A.S., Law, K.H. and Meng, T. (1999), "An experimental study of temperature effect on modal parameters of the Alamosa Canyon Bridge", *Earth. Eng. Struct. Dyn.*, **28**(8), 879-897.

CC